Fracture mechanics parameters evaluation using the digital image correlation technique: a first approach

G. La Rosa, A. Marino Cugno Garrano

Department of Industrial Engineering, University of Catania, Catania (Italy)
glarosa@diim.unict.it

ABSTRACT. The present paper deals with the determination of the critical value of the J-integral by the method of the deep crack on specimens in aluminum 6060 in bending. Following a first step in which the traditional methodologies were used, the Digital Image Correlation (D.I.C.) technique was used in order to determine the Crack Tip Opening Displacement with different values of the crack propagation. The experimental analysis was performed following the three phases of the deep crack methodology: pre-cracking in dynamic conditions, crack propagation under static loading, dynamic failure. The images acquired by the D.I.C. techniques showed values of the CTOD similar to those found with the traditional techniques.

SOMMARIO. Nel presente lavoro è stato determinato il valore critico dell'integrale J mediante il metodo della cricca profonda su provini di alluminio 6060 in flessione. Dopo una prima analisi sulla base delle metodologie tradizionali, è stata usata la Digital Image Correlation (D.I.C.) per determinare il CTOD per differenti valori della propagazione della frattura L'analisi sperimentale è stata eseguita pre-criccando il provino in condizioni dinamiche, quindi procurando la propagazione della cricca in condizioni statiche, infine producendo la rottura sotto carico dinamico. Le immagini acquisite mediante D.I.C. mostrano valori del CTOD simili a quelle rilevate con le tecniche tradizionali.

KEYWORDS. Digital Image Correlation; CTOD; Failure propagation; Deep Crack (SE B) Method.

AIM OF THE WORK

Over half a century, a wide literature showed the studies on the fracture mechanics phenomena either in elastic or elastic-plastic conditions and many parameters were adopted to define the crack behavior and the stress-strain state or the energetic state around the crack. Some of the parameters need to be acquired by complicated measuring systems or derived by others.

The authors, based on their experience on optical techniques and, particularly on the Digital Image Correlation (D.I.C.) methodology, following the experience of other authors, proposed the application of the technique to the measure of the Crack Tip Opening Displacement. This first approach of the authors to the application of the methodology to fracture testing is important to verify the compatibility of the position of the reference points with a reliable measure of the crack tip opening, considering the characteristics of the detecting system and the test procedure.

With this aim, a first series of tests was performed on aluminum specimens, using the single edge-notched bend specimens (SE B) in three point bending tests, following the deep crack method to determine the value of the J-integral.

The experimental analysis was carried out for all the specimens following the three phases of the methodology: pre-cracking in dynamic conditions, crack propagation under static loading, dynamic failure.

Some of the specimens were treated to be processed by the D.I.C. analysis measure the CTOD parameter too, in order to correlate it with those derived by the traditional analysis.

EXPERIMENTAL INVESTIGATION

The experimental setup is composed mainly by the image analysis system and the loading devices.
PixeLink PL-B958F videocamera with a resolution of 1600x1200 pixels at 15fps, with f35 1.9 lens and 10 mm extension ring was used to acquire the imaes. In order to improve the light uniformity, essential for a correct D.I.C. algorithm operation, a LED ring with reflecting light diffuser was set around the lens. The cold light source improves the contrast, making better the crack borders definition.

The load was applied, either in dynamic or static field, by a hydraulic *Instron 8872* testing machine with hydraulic clamps and a ± 25 kN load cell.

In order to apply the static load in three points bending, a suitable support (Fig. 1) was realized using steel beams 6x20x110 mm, connected by bolts to the 170 mm basis beams (box steel section bar 60x40 mm) at a distance of 120 mm, following the ASTM indication [1], and reinforced by angle irons. Measures were defined so that the clip gage could be easily mounted without interference with the loading device. The punch and the supports were rounded with 3 mm radius to limit the wear with the specimen. The support was used only in the second step of the crack; pre-cracking and final failure were performed by tensile cyclic loading.
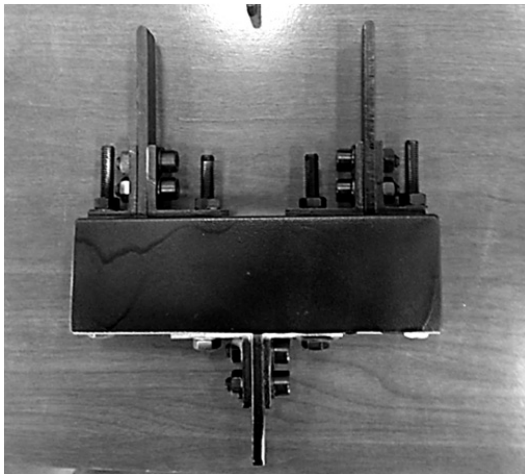
Figure 1: Three points bending device.
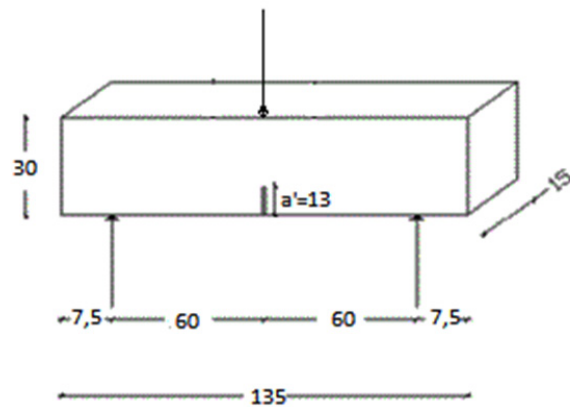
Figure 2: Three points bending specimen.

Following the ASTM indication, the three points bending specimen dimensions are reported in Fig. 2. The cross-sectional area is 30x15 mm^2, the support distance is 120 mm.

All the specimens were in aluminum 6060, whose mechanical characteristics are: σ_Y = 170 MPa, UTS = 205 MPa, E = 70 GPa, ν = 0.327, n_i = 0.18. The characteristics were measured by testing three specimens under static tensile loading by a static testing machine *Zwick-Roell Z100* with a 100 kN load cell in control of displacement at a cross-head speed of 5 mm/min and verifying the results obtained with those derived from literature.

The first notch was realized by a belt saw with a 1 mm blade for a 13 mm initial length. The corresponding stress concentration factor (by literature) was K_t = 2.8.

The opening displacement δ was measured by a 3541-005M-100M-ST *Epsilon Technology Corp.* clip gage, using LabView software [2]. The device was placed between two 30 deg brackets mounted on the specimen, with an 8mm relative distance.

In order to observe the crack growth, a *Micronta Illuminated Microscope* 30x was used. The microscope measured the height b of the cross-sectional area after the pre-cracking phase (b = W – a_0) and the amount of the crack propagation Δa.

The experimental analysis deals with the determination of the stress intensity factor using the Deep Crack Method. The trials were carried out in three phases:
a)   Pre-cracking under cyclic loading;
b)   Crack propagation under static load;
c)   Failure cracking under cyclic loading.

The parameter to be founded is the critical value of the J-integral J_c. It was be defined by the J-Δa diagram, the curve resulting by the interpolation of the points derived by the correspondence between the applied loads P and the respective measured variation of the crack length Δa. By the clip gage measurements and suitable geometrical considerations, then, it is possible defining the J-integral by the Δ displacement as [3-6] $\quad J = 2 \int_0^\delta P \, d\Delta \, /(B \, b)$.

The tests were performed on ten aluminum 6060 specimens, being five the minimum number previous by the standard. Two of them were set for the D.I.C. measurements.

After some failed trials to pre-crack the specimen in bending or in traction under loading control, the pre-cracking phase was carried out applying tensile stress under displacement control at 10 Hz frequency (Fig. 3). The imposed displacement was 0.5 mm for 500 cycles with load ratio R=0.
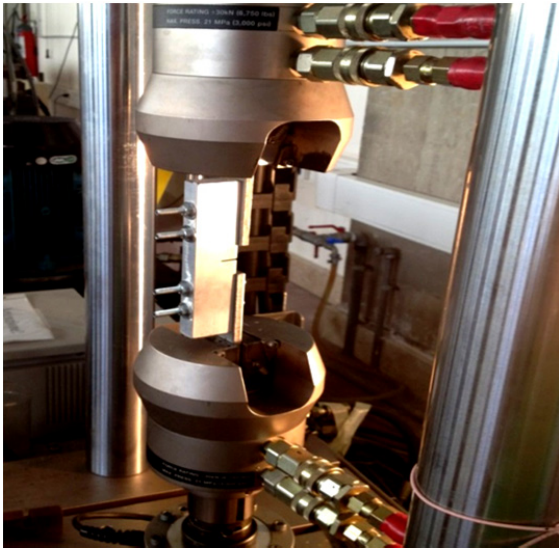
Figure 3: Pre-cracking layout.
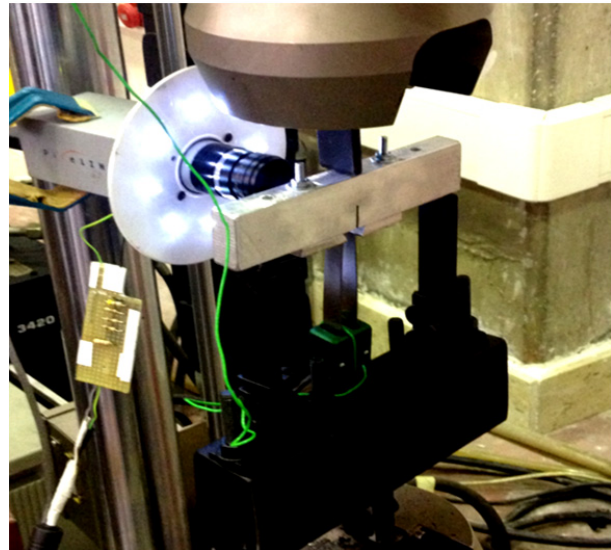
Figure 4: Three points bending layout.

Following the ASTM standard, the range admitted for the initial length *a* must be $0.45 \le a/W \le 0.70$. All the initial crack lengths, reported in Tab. 1, are comprised in the desired range [1].

Specimen No.	b [mm]	a [mm]	a/W	U [N mm]	J [N/mm]	Δa [mm]
1	15.75	14.25	0.475			
2	15.35	14.65	0,488			
3	14.60	15.40	0.513	6038.63	55.15	0.070
4	12.80	17.20	0.573	13817.84	143.94	5.050
5	14.20	15.80	0.527	28688.81	269.38	1.875
6	15.25	14.75	0.518	31655.98	276.77	1.190
7	14.65	15.35	0.548	27318.72	248.63	1.885
8	15.90	14.10	0.530	32042.55	268.70	2.950
9	12.00	18.00	0.600	18100.00	201.11	0.520
10	13.10	16.90	0.563	22414.88	228.14	2.705

Table 1: Geometrical and energetic values for the tested specimens.

The second phase was the crack propagation under static loading. The tests were performed by three points bending. Using the clip gage measurements δ, the total load-line displacements Δ were calculated by geometrical considerations as a function of the applied load P. It was preferred to consider the specimen with a plastic hinge and measuring the crack opening by the clip gauge in order to avoid the testing machine clearances and the support deformations.

By LabView analysis, after the adequate calibration, all the data were correlated to the test time and, then the opening displacements to the corresponding loads. Among the ten specimens, the first two specimens were used to determinate the static load suitable for the application of the methodology and reached the failure for instable propagation of the crack. For the other specimens the curve P - Δ was acquired. As an example, the curve P-δ for the specimens No. 3 and No. 5 are shown in Fig. 5 and 6.
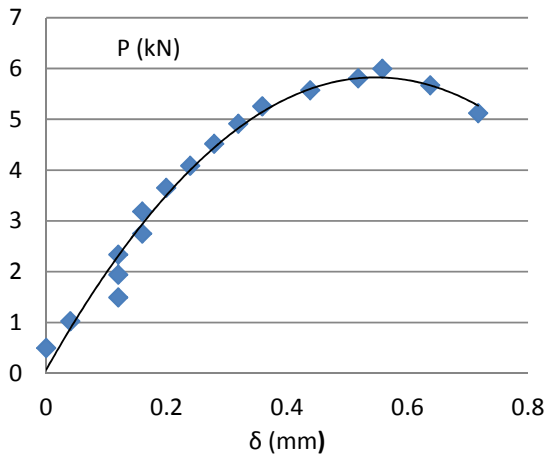
Figure 5: Load-displacement curve for the specimen No.3.
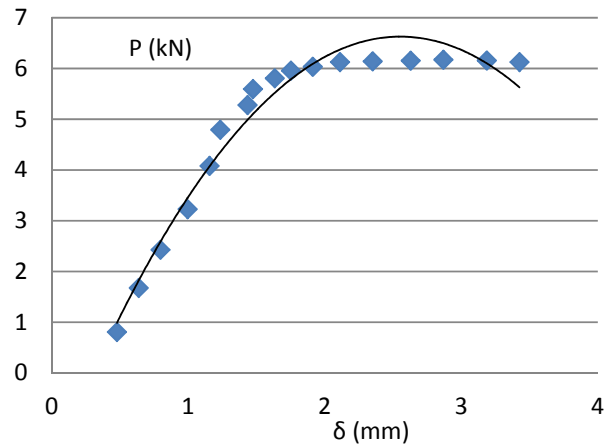
Figure 6: Load-displacement curve for the specimen No.5.

The curves so realized, interpolating by points, show the correlation between the displacement δ and the load P. The areas defined by the curves represent, after the geometrical conversion from δ to Δ, the work U and, then, allow calculating the J-integral, following the expression: $J = 2 \int_0^\delta P \, d\Delta \, /(B \, b) = 2 \, U/(B \, b)$. The results for U and J are reported in Table 1.

During the second phase, moreover, the specimens No. 9 and No. 10 were treated for the D.I.C. analysis and the images were acquired during the whole phase.

After grinding the interested area, specimens No. 9 and No. 10 were firstly sprayed with white paint; then, using the airbrush, a random distribution of black dots, with an average dimension of about 30 μm, was generated by China ink [7]. It is very important that the speckles create a light intensity distribution different for each subset; otherwise the correlation process could fail. The specimens were loaded immediately after the speckle creation, to avoid the drying process. The videocamera was set orthogonally to the specimen at a distance of few centimeters (Fig. 4).

The third phase consists in producing the final failure of the specimens, marking the different zones created by the first two phases. The specimens were subjected once again to cyclic tensile loading, in order to create a fracture surface different than that created by the static propagation. The load ratio R was maintained always positive, in order to avoid that the fractures surfaces could be in contact. The loading machine was set in displacement control at the value of 1 mm at 10 Hz. Failure happened after about 3,000 cycles for almost all the specimens.

Most of the specimens, before being put through the final cyclic tensile loading, were baked in a vinegar bath, in order to highlight the fracture surface. The vapor produced at about 200 °C penetrated deeply inside the fracture, showing a clear separation between the different surfaces (Fig. 8).

The fracture depth was finally measured with great accuracy to define the propagation Δ*a*. Measures on six equidistant points from the border to the center of the specimen were made and the average value was calculated for Δ*a*. The values are reported in Table 1.

From these results it is possible defining the curve J –Δ*a*, showed in Fig. 9. In the same figure the blunting line was also plotted, based on the equation $J = 3.75 \, \sigma_Y \, \Delta a$ [4]. The J_c value was found as intersection between the interpolating curve and the *offset line*, parallel to the blunting line and distant Δ*a* = 0.2 mm. The value found for J_c is about 180 N/mm. The limitation of $J_{lim} = b_0 \, \sigma_Y/10$, where $b_0 = W-a_0$ and a_0 is the sum of the notch length and the initial crack length, defining the zone of validity for the critical parameters was sometimes exceeded, as well as the condition *a*, B, W-*a* ≥ 25 J_c/σ_Y. Then, the evaluation of the parameters J_c and, consequently, K_{Ic} cannot be considered reliable. In any case, in the aim of the present paper, the correspondence between J and CTOD could be still considered.

Figure 7: Two specimens at the end of the second phase.
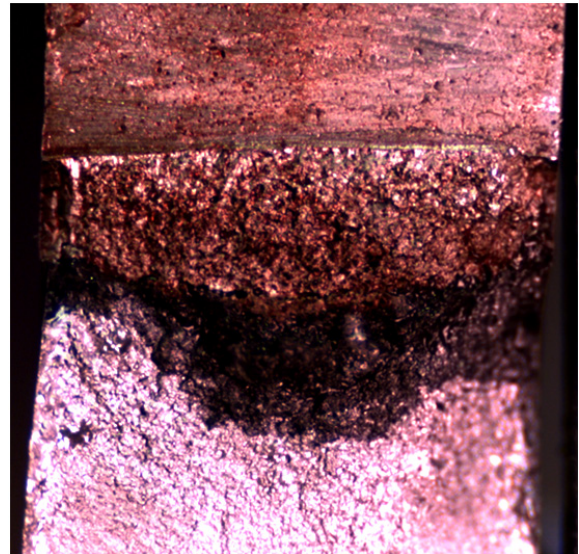
Figure 8: Fracture surface after vinegar baking.
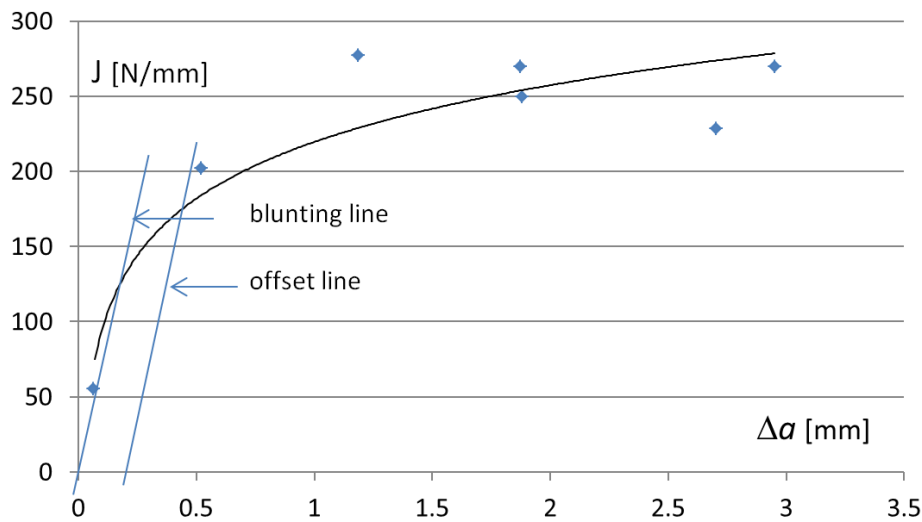
Figure 9: J-R curve.

DIGITAL IMAGE CORRELATION ANALYSIS

The D.I.C. analysis [7-12] was carried out regarding the second phase of loading, therefore the static propagation under three points bending.

During the first phase (cyclic tensile loading) only two images were acquired, before and after the crack generation. For these images, after conversion in grey scale (Fig. 10), the analysis was performed using the *MOIRE* software. Thanks to the dots correlation, it was possible to derive the displacements and, consequently, the strain state. The results are reported in Fig. 11 to 13, showing the displacements and the strain along the horizontal and vertical axis, respectively. The colored area represents the region of interest (ROI) where the process was carried out. Fig. 11, in particular, shows the two different zones (yellow-green and violet-blue) being opposite the sign of the displacements.

In order to correlate the images acquired at the end of the static three points bending, the Matlab software were used, the process was dedicated to define the Crack Tip Opening Displacement (CTOD) at a determinate distance from the fracture tip. After converting the image in b/w, a reference grid was defined (Fig. 14).

The CTOD value δ was calculated for both the grid columns, considering the relative sum of the displacement for each upper grid point with the corresponding point of the lower grid. For each value of y, defined as the distance of the interest

points grid on the same column, a value of the CTOD, depending on the distance of point columns from the fracture tip, was calculated. The distances chosen for the two specimens (No. 9 and No. 10) are reported in Table 2.

Figure 10: Initial crack in the speckled specimen (visible).
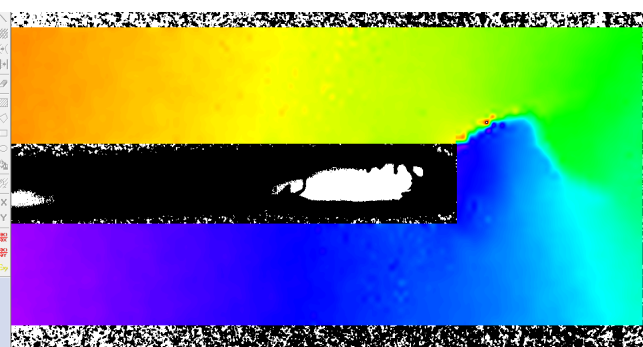
Figure 11: Displacements in the ROI zone.
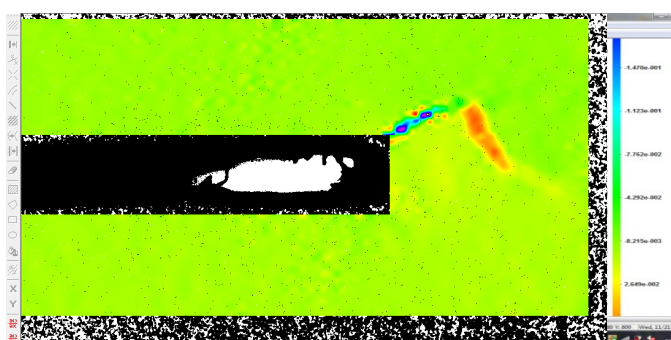
Figure 12: Horizontal strain in the ROI zone.
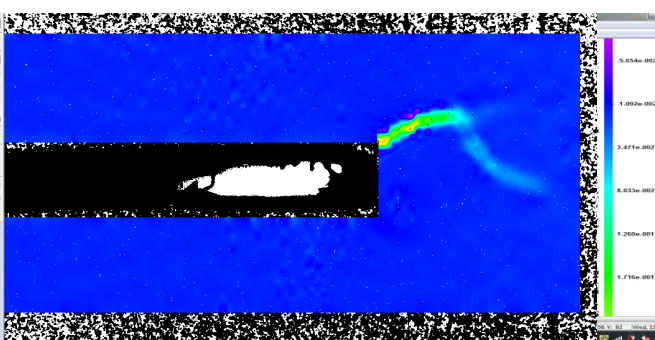
Figure 13: Vertical strain in the ROI zone.
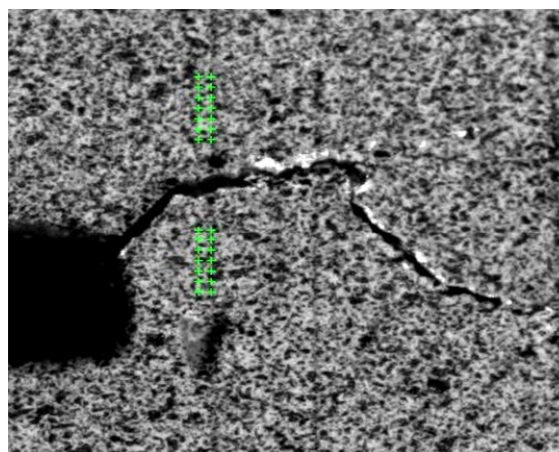
Figure 14: Grid position.

Specimen No. 9 [pixels]	Specimen No.10 [pixels]
x'= 281	x'= 173
x"= 271	x"= 163

Table 2: Distances from the fracture tip.

The grid must contain the central points of the subsets to be analyzed by the correlation software, giving their position for each frame. Defined grid has two columns and seven rows, a total of 14 central points at a distance of 10 pixels (1 pixel ≈

11μm). Therefore, the subsets for the correlation analysis have an area of 10x10 pixels. In order to calculate the CTOD, a symmetrical grid on the opposite site of the fracture line has to be realized. The choice of two grids of seven points each came from the image size and from the need to verify the stability of the measurements between the symmetrical couples of points.

Then, the correlation among the areas was processed. During the processing time (about one second per image), the displacements of the grid points could be followed and recorded on two matrices.

For the different points, the results are shown in Fig. 15. These show that the displacements of the selected subsets at low distances along the vertical run in an almost stationary way, then the value found for each couple of points at the same distance offers a high precision for this analysis.
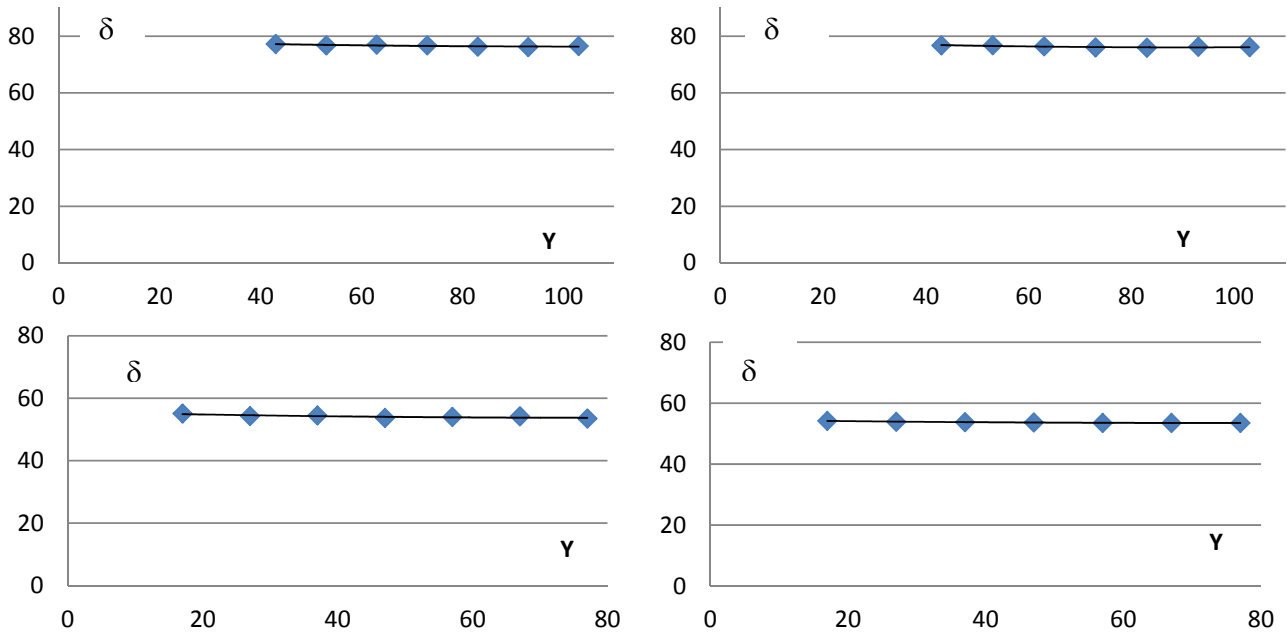
Figure 15: Values of the CTOD δ along the grid points for the specimen No. 9 (upper) at x'=281 (left) and x''=271 (right) and for the specimen No. 10 (lower) at x'=173 (left) and x''=163 (right), respectively. Values are in pixels (1 pixel ≈ 11 μm).

Finally, a comparison was made between the values found for the CTOD δ and those for J, following the expression [4, 5] $J_\delta = m\ \sigma_Y\ \delta$, in which the constraint factor m has a value between 1 and 2 (m=1 for plane stress state, m = 2 for plane strain state). Considering the narrow plastic zones (Fig. 7 and 8) but the limitations about the thickness previously discussed, the value of m could be considered between 1.5 and 2. The J calculated values by the deep crack method (J_U) are reported in Table 3 together with those calculated by the CTOD methodology (J_δ) using the D.I.C. measurements. Even if on two specimens only, the results are in acceptable agreement.

Specimen No.	δ [mm]	$J_{\delta\ max}$ [N/mm]	$J_{\delta\ min}$ [N/mm]	J_U [N/mm]
9	0.8	272.0	204.0	201.11
10	0.6	204.0	153.0	228.14

Table 3: Comparison between expected and calculated J.

CONCLUSIONS

The paper presented the results obtained by a series of test performed on notched specimens in aluminum 6060 to define the fracture mechanics parameters. The analysis was realized using traditional methodologies and by the application of the D.I.C. technique.

The study could be formally subdivided in an experimental phase and two different data processing procedures. On the tested specimens it was possible to follow an experimental procedure allowing reliable measurements. The J-integral parameter was defined by the deep crack method on specimens pre-cracked by cyclic tensile loading and, in a second phase, subjected to static three points bending.

Using the D.I.C. technique it was also possible to calculate the CTOD in different positions respect to fracture tip. The results obtained, considering points vertically aligned, very close and symmetrical respect the fracture line, allow evaluating the parameter with good precision and permitting to consider it as a reliable measuring technique.

Finally, the results obtained using the traditional deep crack SE (B) methodology were compare with those derived by the D.I.C. measurements, showing an acceptable agreement.

REFERENCES

[1]   ASTM E 1820: Standard test method for measurement of fracture toughness (2001).

[2]   G. Mirone, D. Corallo, Engineering Fracture Mechanics 102 (2013) 18.

[3]   V. Crupi, E. Guglielmino, M. Labanti, S. Merenda, In: XVIII Convegno Nazionale IGF, Cetraro (CS, Italy) (2006).

[4]   L. Vergani, Meccanica dei materiali, McGraw-Hill (2001).

[5]   X.-K. Zhu, J.A. Joice, Engineering Fracture Mechanics, 85 (2012) 1.

[6]   J. Lemaitre, J.L. Chaboche, Mécanique des materiaux solides, Dunod (1988).

[7]   A. Marino Cugno Garrano, G. La Rosa, D. Zhang, L.N. Niu, F.R. Tay, H. Majd,D. Arola, Journal of the Mechanical Behavior of Biomedical Materials, 7 (2012) 17.

[8]   M. A. Sutton, J.J. Orten, H.W. Schreier, Image Correlation for Shape, Motion and Deformation Measurements – Basic Concepts, Theory and Applications, Springer (2009).

[9]   L.C.S. Nunes, J.M.L. Reis, H.S. da Costa Mattos, Engineering Fracture Mechanics, 78 (17) (2011) 2957.

[10] P. Leplay, J. Réthoré, S. Meille, M.C. Baietto, International Journal of Fracture, 171 (1) (2011) 35.

[11] J. Carroll, C. Efstathiou, J. Lambros, H. Sehitoglu, B. Hauber, S. Spottswood, R. Chona, Engineering Fracture Mechanics 76 (15) (2009) 2384.

[12] J.R. Yates, M. Zanganeh, Y.H. Tai, Engineering Fracture Mechanics, 77 (11) (2010) 2063.

[13] W.T. Riddell, R.S. Piascik, M.A. Sutton, W. Zhao, S.R. McNeill, J.D. Helm, In: Advances in fatigue crack closure measurements and analysis, R.C. McClung and J.C. Newman Jr. Editors, 157-174 (1999), ASTM STP 1343.